MIT Open Access Articles

Correcting Microwave Precipitation Retrievals for near-Surface Evaporation

Massachusetts Institute of Technology

CORRECTING MICROWAVE PRECIPITATION RETRIEVALS FOR NEAR-SURFACE EVAPORATION

Chinnawat Surussavadee[1,2], Member, IEEE, and David H. Staelin[1], Life Fellow, IEEE

[1]Research Laboratory of Electronics, Massachusetts Institute of Technology, Cambridge, MA 02139 USA

[2]Andaman Environment and Natural Disaster Research Center, Faculty of Technology and Environment, Prince of Songkla University, Phuket Campus, Phuket 83120 Thailand

ABSTRACT

This paper compares two methods for correcting passive or active microwave surface precipitation estimates based on hydrometeors sensed aloft that may evaporate before landing. These corrections were derived using two years of data from 516 globally distributed rain gauges and passive millimeter-wave Advanced Microwave Sounding Units (AMSU) aboard three NOAA satellites (N15, N16, and N18). The first correction reduces rms differences between rain gauges and AMSU annual precipitation accumulations (mm) by a separate factor for each infrared-based surface classification, while the second correction factor uses a 3-2-1 neural network (NN) trained using both surface classification and annual average relative humidity profiles. Different data were used for training and accuracy evaluation. The NN results agreed with rain gauges better than did surface classification corrections alone. The rms annual accumulation errors relative to the 516 uncorrected rain gauges using AMSU with surface classification and NN corrections were 223 and 209 mm/yr, respectively, compared to 152 mm/yr for GPCP, which incorporates rain gauge data and data from more satellite sensors.

Index Terms—Advanced Microwave Sounding Unit (AMSU), microwave precipitation estimation, precipitation, evaporation, rain, remote sensing, satellite, snow, virga.

1. INTRODUCTION

Almost all active and passive microwave remote sensing systems estimate precipitation by sensing hydrometeor populations that may partially evaporate while typically falling more than a kilometer before reaching the ground. Two methods for correcting microwave precipitation retrievals for such evaporation were evaluated and could be adapted to any satellite or ground-based microwave precipitation sensor, active or passive. One correction method uses land surface classification and the other is based on both land surface classification and relative humidity statistics. The methods were developed by reconciling two years of passive millimeter-wave surface precipitation estimates [1]-[6] from the Advanced Microwave Sounding Unit (AMSU) on the U.S. NOAA-15, -16, and -18 operational weather satellites with 516 globally distributed rain gauges [7]. Evaporation-corrected surface precipitation estimates from the two methods were evaluated using rain gauges and were compared with Global Precipitation Climatology Project (GPCP) estimates [8].

2. AMSU MIT PRECIPITATION RETRIEVAL ALGORITHM (AMPR)

The AMSU MIT Precipitation Retrieval algorithm (AMPR) utilizes 13 channels spaced from 23 to 191 GHz and was trained using the fifth-generation National Center for Atmospheric Research/Penn State Mesoscale Model (MM5) [1]-[6]. AMPR version 3 (AMPR-3) has successfully mapped precipitation over the North Pole and elsewhere, the principal remaining limitation being high elevation land like the Himalayan, Greenland, and Antarctic plateaus, and major mountain chains like the Andes [5]. Confirmation of the plausibility of these retrievals was obtained by comparisons with CloudSat 94-GHz radar and annual surface precipitation rate maps from the Global Precipitation Climatology Project (GPCP) [5]-[6].

Although average annual accumulations (mm/yr) observed in 2006-2007 by 787 globally distributed rain gauges located in non-hilly regions (defined as those for which the surface elevation varied by more than 500 m within a box of ±0.2º of longitude and latitude) reasonably agreed for most surface classifications with AMPR-3 retrievals, AMPR-3 significantly overestimated precipitation for under-vegetated land. The ratios of these AMPR-3 annual accumulations to those of gauges ranged from 0.88 for tundra to 1.37 for cultivated crops, while the ratios for grassland, shrubs over bare ground, and pure bare ground (desert) were 2.4, 3.1, and 9, respectively, suggesting significant evaporation at altitudes beneath those of the hydrometeors sensed by AMSU. MM5 simulations strongly suggest that rain evaporation is largely responsible [6].

3. EVAPORATION CORRECTION METHODS

Two near-surface evaporation correction methods were developed and evaluated, including one based only on land

classification and the other based on both land classification and annual relative humidity.

3.1. Correction method based on land classification

AMPR-3 surface precipitation retrievals for NOAA-15, -16, and -18 were averaged into a 1-degree grid separately for years 2006 and 2007. The annual totals (mm/yr) were then computed and interpolated to rain gauge locations. The evaporation correction for this first method is the bias ratio, which is defined as the ratio between the annual means of the AMPR-3 and rain gauge annual accumulations (mm/yr) within each surface classification, independent of season and location within each region.

The surface classifications were deduced from the Advanced Very High Resolution Radiometer (AVHRR) infrared spectral images [9]. Since many coastlines have significant undulations and therefore uncertain emissivity per pixel, rain gauge sites within 55 km of a coastline were classed separately as "coastline" instead of using the AVHRR surface classification. Latitudes above 75ºN were also defined as a separate class.

To develop and evaluate near-surface evaporation correction methods, this paper uses 516 rain gauges located in non-hilly and non-coastal sites, which are a subset of the gauges used in [6]. The coastal sites were not used because their biases and errors are mostly due to emissivity uncertainties unrelated to evaporation.

The ratio-correction maps at 1-degree resolution were computed separately for years 2006 and 2007 and were applied to the AMPR-3 surface precipitation rate retrievals, yielding the AMPR-4 retrievals [6].

3.2. Correction method based on land classification and relative humidity

Surface classification, however, does not fully reveal global atmospheric variations or predict variations over ocean or large lakes where gauges are not available.

In Fig. 1, pluses show correlation coefficients between the base-10 logarithm of observed AMPR-3/gauge annual accumulation ratios and 19 variables including in numerical order: the surface classification, the base-10 logarithm of AMPR-3 annual precipitation, and the base-10 logarithm of annual average relative humidity for 17 pressure levels (1000, 975, 950, 925, 900, 850, 800, 750, 700, 650, 600, 550, 500, 450, 400, 350, and 300 mb). The correlation coefficients were shown separately for rain gauge annual accumulations ≤ 2000 mm/yr (red pluses), > 2000 mm/yr (blue pluses), and > 900 mm/yr (green pluses). The squares in Fig. 1 represent the correlation coefficients between the base-10 logarithm of AMPR-3 annual precipitation and the 19 variables, where self-correlations were not plotted. Red, blue, and green squares are for gauge annual accumulations ≤ 2000 mm/yr, > 2000 mm/yr, and > 900 mm/yr, respectively. The relative humidity data are from the U.S.

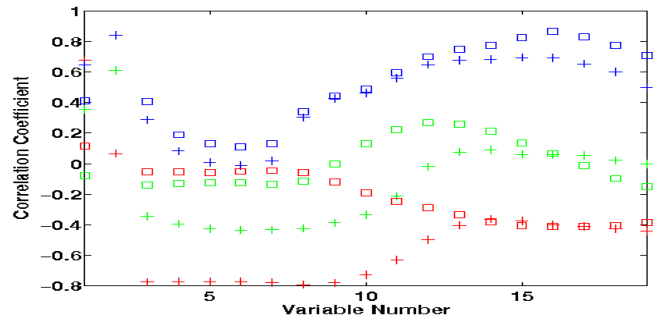National Center for Environmental Prediction (NCEP) analyses at ~110-km resolution.

Fig. 1. Pluses: correlation coefficients between the base-10 logarithm of observed AMPR-3/gauge ratios and 19 variables for 516 gauges that are non-hilly and non-coastal. Squares: correlation coefficients between the base-10 logarithm of AMPR-3 annual precipitation and the 19 variables. Red, blue, and green symbols indicate gauges ≤ 2000 mm/yr, gauges > 2000 mm/yr, and gauges > 900 mm/yr, respectively.

The high values for Variable 1 in Fig. 1 show that AMSU/gauge ratios (red pluses) are highly correlated with surface classification whereas those same ratios are poorly correlated with AMPR-3 annual precipitation (Variable 2) for gauges ≤ 2000 mm/yr. Whereas AMSU/gauge ratios for gauges ≤ 2000 mm/yr have highly negative correlations with average annual relative humidity for altitudes below ~750 mb (red pluses for variables 3-10), AMPR-3 accumulations (red squares) are nearly uncorrelated. These highly negative correlations between AMSU/gauge ratios and low-altitude relative humidity are due to drier air at low altitudes that evaporates rain and reduces gauge measurements, thus increasing the AMSU/gauge ratios. Since the high AMSU/gauge ratios are apparently due to near surface evaporation by dry air, relative humidity data provides an additional means for correcting surface precipitation-rate retrievals for evaporation. Unlike surface classification alone this correction method also extends over ocean.

Since the correlation coefficients between high-altitude relative humidity and both AMSU/gauge ratios and AMPR-3 accumulations are approximately the same, this correlation is not due to near surface evaporation.

The ratio correlations (blue pluses) in Fig. 1 for gauges reporting over 2000 mm/yr also suggest that relative humidity below 750 mb (variables 3-10) is much less informative then because evaporation is less important in those humid tropical regions. Also, since low-altitude humidity is comparably correlated with both AMPR-3 annual accumulations and AMSU/gauge ratios for sites > 2000 mm/yr, it follows that near-surface evaporation has less effect on AMSU/gauge ratios when the precipitation is strong; high relative humidity then contributes little information about near-surface evaporation.

The second method uses a 3-2-1 neural network (NN) to estimate the evaporation correction, where its inputs are the 19 variables. NNs were trained to estimate the base-10 logarithm of observed AMPR-3/gauge annual accumulation

ratios. Annual observations for years 2006 and 2007 from 516 rain gauges that are non-hilly and non-coastal were used for training and evaluation. Gauge observations with extreme gauge/AMSU ratios, ≤ 0.3 or ≥ 20, were not used for training AMPR-4 and AMPR-5, but they were used for evaluation.

To help prevent NNs from learning event-specific discrepancies that could lead to potentially optimistic estimates of performance, the two-year dataset was separated into two independent sets, each randomly having half the gauges for 2006 and 2007. The best of 200 neural networks (the one with the lowest rms error) was selected for each set, where 50 percent of each set was used for training, 25 percent for validation, and 25 percent for testing. These two best NNs were then each tested on the full opposite and independent set of observations, and the estimated AMPR-5 annual accumulation retrieval accuracies are presented in Table I. The same two-set two-year accuracy estimation strategy was also used for AMPR-4.

Since near-surface relative humidity is not very useful for estimating evaporation when annual accumulations are greater than 2000 mm/yr, AMPR-4 correction ratios were used instead when AMPR-4 estimates exceeded 2000 mm/yr. The 1-degree correction maps derived separately for years 2006 and 2007 were applied to the AMPR-3 surface precipitation rate retrievals, yielding the AMPR-5 retrievals.

4. RESULTS

AMPR-3 [5], AMPR-4 [6], AMPR-5, and GPCP were compared to wind-loss-uncorrected gauge annual accumulations (mm/yr) in Fig. 2 for all 516 non-hilly and non-coastal gauges for years 2006 and 2007. It shows that AMPR-4 and AMPR-5 perform much better than AMPR-3 and that AMPR-5 performs better than AMPR-4. Moreover the AMPR-5 corrections apply over ocean. Both the scatters and biases were reduced. The GPCP analyses agree artificially well with uncorrected gauges having low annual accumulations because the wind-loss corrections were removed from these GPCP data and GPCP incorporates rain gauge measurements from the Global Precipitation Climatology Centre (GPCC) gauge analyses when satellite data are less reliable, e.g., in dry climates. The wind-loss adjustment was not used for gauges in this paper because existing global wind-loss adjustments are quite outdated.

Table I presents rms errors, biases (estimate − gauge), and correlation coefficients for AMPR-3, AMPR-4, AMPR-5, and GPCP relative to all gauge annual observations, and separately for gauge annual accumulations ≤ 900 mm/yr and > 900 mm/yr. The results show that both AMPR-4 and AMPR-5 greatly improve AMPR-3. By using near-surface evaporation information inferred from annual averages of relative humidity, AMPR-5 performs better than AMPR-4 in terms of rms errors and correlation coefficients. AMPR-4 has less bias than AMPR-5 because the AMPR-4 land-class correction ratios were tuned to make the expected biases

zero. AMPR-5 reduces rms errors of AMPR-3 by 60.6 and 22.2 percent for gauge annual accumulations ≤ 900 mm/yr and > 900 mm/yr, respectively. Biases and correlations were also substantially improved. Although the 209-mm/yr rms errors for AMPR-5 are approaching the GPCP 152-mm/yr rms discrepancies, there is considerable room for improvement even though the GPCP data are artificially good because they incorporate to some degree the reference rain gauge data and precipitation estimates from more satellites. The large bias between GPCP and the 516 unadjusted reference rain gauges was removed here by undoing the GPCP rain-gauge wind-loss adjustments. The GPCP correlation coefficient for gauge annual accumulations ≤ 900 mm/yr is artificially high due to the GPCC rain-gauge analyses used in GPCP that particularly affect sites with little rain.
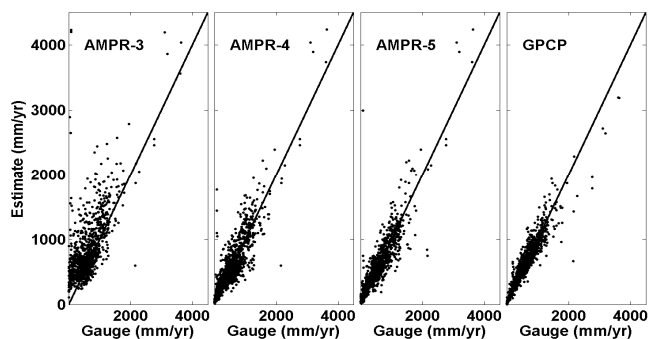

Fig. 2. Scatter plots of AMPR-3, AMPR-4, AMPR-5, and GPCP versus gauge annual precipitation accumulations.

TABLE I
RMS ERRORS, BIASES (ESTIMATE − GAUGE), AND CORRELATION COEFFICIENTS FOR AMPR-3, AMPR-4, AMPR-5, AND GPCP FOR 516 GAUGE ANNUAL OBSERVATIONS

Estimate		AMPR-3	AMPR-4	AMPR-5	GPCP
RMS Error	All	433.59	223.39	209.46	151.62
	≤ 900 mm/yr	439.61	191.07	173.29	112.63
	> 900 mm/yr	407.91	323.96	317.43	255.60
Bias	All	206.95	15.18	17.09	20.66
	≤ 900 mm/yr	219.12	28.20	36.10	46.81
	> 900 mm/yr	156.92	-38.31	-61.00	-86.80
Corr. Coef.	All	0.66	0.86	0.88	0.93
	≤ 900 mm/yr	0.20	0.67	0.75	0.91
	> 900 mm/yr	0.74	0.81	0.83	0.83

Fig. 3 shows global maps of 2-yr mean annual precipitation discrepancies (estimate − gauge) between 516 gauges and AMPR-3, AMPR-4, AMPR-5, and (after removal of gauge wind-loss corrections) GPCP. AMPR-4 and AMPR-5 provide much improvement over AMPR-3, and AMPR-5 particularly improves the results over the central U.S.A. and south-east Australia. Some sites pose

special problems for AMPR such as the Australian dry lake; these can be individually addressed in the future.

The somewhat regional character of these biases suggests they may have geophysical origins that future gauge and algorithm adjustments can reduce.

5. SUMMARY AND CONCLUSION

Two near-surface evaporation correction methods were developed for microwave precipitation sensors and were used in AMPR-4 and AMPR-5. AMPR-4 employed evaporation information from surface classification alone, whereas relative humidity profiles were also used in AMPR-5. Both greatly reduce the errors due to evaporation below the remotely sensed hydrometeors. AMPR-5 performs better than AMPR-4 and is approaching GPCP, which incorporates rain gauge data and data from more satellite sensors. Rain evaporation correction factors can be derived for other types of microwave precipitation observations by regressing annual relative humidity against the discrepancies between the microwave observations and the rain gauges. Such evaporation corrections would differ among instruments that sense different functions of the hydrometeor distribution with altitude.

6. REFERENCES

[1] C. Surussavadee and D. H. Staelin, "Comparison of AMSU Millimeter-Wave Satellite Observations, MM5/TBSCAT Predicted Radiances, and Electromagnetic Models for Hydrometeors," *IEEE Trans. Geosci. Remote Sens.*, vol. 44, no. 10, pp. 2667-2678, Oct. 2006.
[2] C. Surussavadee and D. H. Staelin, "Millimeter-Wave Precipitation Retrievals and Observed-versus-Simulated Radiance Distributions: Sensitivity to Assumptions," *J. Atmos. Sci.*, vol. 64, no. 11, pp. 3808-3826, Nov. 2007.
[3] C. Surussavadee and D. H. Staelin, "Global Millimeter-Wave Precipitation Retrievals Trained with a Cloud-Resolving Numerical Weather Prediction Model, Part I: Retrieval Design," *IEEE Trans. Geosci. Remote Sens.*, vol. 46, no. 1, pp. 99-108, Jan. 2008.
[4] C. Surussavadee and D. H. Staelin, "Global Millimeter-Wave Precipitation Retrievals Trained with a Cloud-Resolving Numerical Weather Prediction Model, Part II: Performance Evaluation," *IEEE Trans. Geosci. Remote Sens.*, vol. 46, no. 1, pp. 109-118, Jan. 2008.
[5] C. Surussavadee and D. H. Staelin, "Satellite Retrievals of Arctic and Equatorial Rain and Snowfall Rates using Millimeter Wavelengths," *IEEE Trans. Geosci. Remote Sens.*, vol. 47, no. 11, pp. 3697-3707, Nov. 2009.
[6] C. Surussavadee and D. H. Staelin, "Global Precipitation Retrievals Using the NOAA/AMSU Millimeter-Wave Channels: Comparison with Rain Gauges," *J. Appl. Meteorol. Climatol.*, vol. 49, no. 1, pp. 124-135, Jan. 2010.
[7] NOAA, cited 2007: Monthly climatic data for the world. [Available at http://www7.ncdc.noaa.gov/IPS/mcdw/mcdw.html.]
[8] G. J. Huffman, R. F. Adler, M. M. Morrissey, D. T. Bolvin, S. Curtis, R. Joyce, B. McGavock, and J. Susskind, "Global precipitation at one degree daily resolution from multisatellite

observations," *J. Hydrometeor.*, vol. 2, no. 1, pp. 36–50, Feb. 2001.
[9] M. C. Hansen, R. S. DeFries, J. R. G. Townshend, and R. Sohlberg, "Global land cover classification at 1 km spatial resolution using a classification tree approach," *Int. J. Remote Sens.*, vol. 21, pp. 1331–1364, 2000.
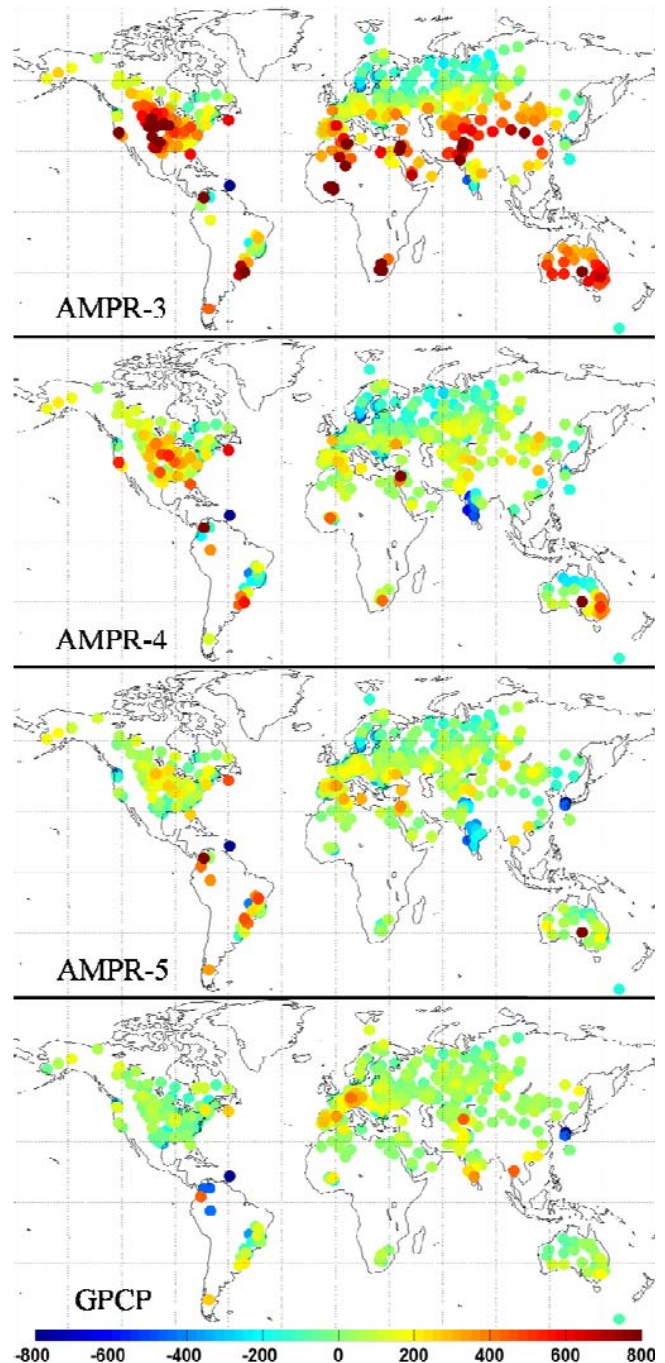
Fig. 3. Global maps of 2-yr mean annual precipitation error (estimate – gauge) for AMPR-3, AMPR-4, AMPR-5, and (after removal of gauge wind-loss corrections) GPCP for 516 wind-loss uncorrected gauge observations.